

# Modelling variability in lymphatic filariasis: macrofilarial dynamics in the *Brugia pahangi*–cat model

E. Michael<sup>1\*</sup>, B. T. Grenfell<sup>2</sup>, V. S. Isham<sup>3</sup>, D. A. Denham<sup>4</sup> and D. A. P. Bundy<sup>1</sup>

<sup>1</sup>Department of Zoology, University of Oxford, South Parks Road, Oxford OX1 3PS, UK

<sup>2</sup>Department of Zoology, University of Cambridge, Downing Street, Cambridge CB2 3EJ, UK

<sup>3</sup>Department of Statistical Science, University College London, Gower Street, London WC1E 6BT, UK

<sup>4</sup>The London School of Hygiene and Tropical Medicine, Keppel Street, London WC1E 7HT, UK

A striking feature of lymphatic filariasis is the considerable heterogeneity in infection burden observed between hosts, which greatly complicates the analysis of the population dynamics of the disease. Here, we describe the first application of the moment closure equation approach to model the sources and the impact of this heterogeneity for macrofilarial population dynamics. The analysis is based on the closest laboratory equivalent of the life cycle and immunology of infection in humans—cats chronically infected with the filarial nematode *Brugia pahangi*. Two sets of long-term experiments are analysed: hosts given either single primary infections or given repeat infections. We begin by quantifying changes in the mean and aggregation of adult parasites (inversely measured by the negative binomial parameter,  $k$  in cohorts of hosts using generalized linear models). We then apply simple stochastic models to interpret observed patterns. The models and empirical data indicate that parasite aggregation tracks the decline in the mean burden with host age in primary infections. Conversely, in repeat infections, aggregation increases as the worm burden declines with experience of infection. The results show that the primary infection variability is consistent with heterogeneities in parasite survival between hosts. By contrast, the models indicate that the reduction in parasite variability with time in repeat infections is most likely due to the ‘filtering’ effect of a strong, acquired immune response, which gradually acts to remove the initial variability generated by heterogeneities in larval mortality. We discuss this result in terms of the homogenizing effect of host immunity-driven density-dependence on macrofilarial burden in older hosts

**Keywords:** *Brugia pahangi*, filariasis, macrofilarial dynamics, heterogeneity, moment closure equations, parasite immunity

## 1. INTRODUCTION

A key feature of the ecology of helminth macroparasites is the dispersion pattern of parasite burden between hosts (Anderson & May 1991). Parasites are generally distributed patchily within the host population. This leads to characteristically aggregated frequency distributions of worm burdens, which are often well-fitted empirically by a negative binomial distribution, in which the variance significantly exceeds the mean (Pielou 1977; Anderson & May 1991; Shaw & Dobson 1996). There has been intensive research on parasite aggregation, both in terms of its ecological causes (Croll 1983; Wasson *et al.* 1986; Scott 1987; Quinnell & Keymer 1990) and its consequences for the population dynamics of hosts and parasites (Anderson & Gordon 1982; Pacala & Dobson 1988; Medley 1992). The next major theoretical challenge—to model both the causes and consequences of aggregation simultaneously—remains a formidable problem (Grenfell *et al.* 1995a).

Progress can be made in this area by explicitly considering the demographic processes that generate parasite variability (Anderson & Gordon 1982; Haderl & Dietz 1983; Kretschmar 1989; Kretschmar & Adler 1993; Isham 1995; Grenfell *et al.* 1995a,b). A promising recent approach is to model the dynamics of the second moments of the parasite distribution (essentially the variance–covariance matrix of parasite burden at different stages), as well as the mean. The resulting moment closure equations (MCEs) (Grenfell *et al.* 1995a,b) track levels of parasitism and immunity in a cohort of hosts. In principle, this formulation can be extended to a partial differential equation framework, reflecting the overall dynamics of parasite variability with host age and time. However, in practice, a number of factors complicate this picture. First, the models need to ‘complete the circle’ and model variability in transmission (which both determines and is generated by aggregation of adult worms). Second, we should ideally allow for the prevalence of infection as well as its intensity—current MCEs consider only the latter. We do not consider these problems further in this paper, instead, we focus on the problem of host heterogeneity.

\*Author for correspondence (edwin.michael@zoo.ox.ac.uk).

A large body of work underlines the importance of between-host heterogeneities in response to parasitism in determining both absolute levels of parasite aggregation and patterns of aggregation with host age (Anderson & Gordon 1982; Dietz 1982; Pacala & Dobson 1988; Grenfell *et al.* 1995*a,b*; Isham 1995). Such patterns are hard to quantify in the field and would lead to a great increase in the complexity of analytical models.

One way to approach this problem is to begin by modelling parasite aggregation in laboratory infections—this has the added advantage that we are then considering only the dynamics of parasites in a single cohort of hosts (Crombie & Anderson 1985; Berding *et al.* 1986; Grenfell *et al.* 1987*a,b*). Grenfell *et al.* (1995*b*) recently carried out such an exercise for the relatively simple and epidemiologically well documented interaction between sheep and their gastrointestinal nematode parasites. They found that the aggregation of adult parasites increased significantly under conditions of repeated reinfection and used models to show that this was consistent with between-host heterogeneities in immunocompetence.

A much more challenging problem for the analysis of variability is presented by lymphatic filariasis. Filarial worms are the most important human macroparasites transmitted by mosquitoes—persistent infection causes significant ocular (onchocerciasis) and lymphatic pathology (lymphatic filariasis) in large areas of the tropics (WHO 1987; Michael *et al.* 1996). Understanding the causes and consequences of variability is a particular problem for these infections, especially for lymphatic filariasis (Grenfell *et al.* 1990). Infective larvae are transmitted to humans by mosquitoes and develop into adult worms (macrofilariae) in the lymphatics. Eggs from adult females develop into microfilariae, which infect mosquitoes from the peripheral blood circulation. The main problem in quantifying variability is that, despite promising advances in immunodiagnosis (Weil 1990; More & Copeman 1990; Turner *et al.* 1992) and ultrasound scanning (Amaral *et al.* 1994; Dreyer *et al.* 1994), it is still very difficult to quantify the macrofilarial burden. The main tool in the field has been indirect measurement of parasite load, via the density or prevalence of microfilariae in the blood. These microfilarial counts are highly aggregated and teasing out the underlying macrofilarial aggregation from sampling errors and microfilarial dynamics is very difficult (Park 1988; Grenfell *et al.* 1990).

The main problem with the consequences of variability in lymphatic filariasis is concerned with the evaluation of control programmes. There is still no effective macrofilaricide (Ottesen 1994; Ottesen & Ramachandran 1995), so that control programmes aim to interrupt the chain of infection using microfilarial drugs or vector control. The impact of control on the level and persistence of infection in communities therefore depends on the relatively long life span of adult worms in the lymphatics. Given the inherent variability in worm survivorship, host immunity, levels of residual transmission, as well as the above mentioned difficulties in counting adult worms, it is important to allow for variability when modelling the effects of control programmes. The main previous approach, for both onchocerciasis and lymphatic filariasis has been the construction of complex simulation models (Plaisier *et al.* 1990; Remme *et al.* 1995). These formulations

reflect the observed effects of control well; however they are not sufficiently analytically tractable for a general analysis of the determinants of parasite variability.

This paper is the first application of the moment closure approach to lymphatic filariasis. By analogy with Grenfell *et al.* (1995*b*), we begin by modelling the relatively controlled data arising from experimental infections. This allows us to focus directly on macrofilarial counts from dissections, rather than indirect assessment from microfilarial counts. We base the analysis on the closest laboratory analogy to the life cycle and immunology of infection in humans: cats infected with the filarial nematode *Brugia pahangi* (Denham & Fletcher 1987). Specifically, we use generalized linear models to quantify changes in the mean and degree of aggregation of adult parasites in cohorts of hosts, then apply simple stochastic models to interpret these patterns. The analysis is based on long-term macrofilarial infections, following both a single primary infection with larvae (PI), as well as after repeated exposures (RI). Analysing both these cases gives us a picture of the interaction of variability and immunity against previous infections. We begin by introducing the data set, statistical methods and models, then describe and discuss the results of the analyses.

## 2. METHODS

### (a) *Data and experimental methods*

#### (i) *The data*

The principal data set constitutes several series of long-term PI and RI experiments described by Denham *et al.* (1972*a,b*, 1983) and Suswillo *et al.* (1982). Relevant unpublished records of cat infections were also used for analyses. A subpopulation of cats spontaneously lose their microfilariae and become immune to subsequent infection (Denham & Fletcher 1987; Grenfell *et al.* 1991; Denham *et al.* 1992). Analysis of this form of acute immunity will be presented in a future paper. Here, attention is restricted mainly to those 'susceptible' cats that carried chronic, nonsymptomatic microfilarial infections for the duration of both single and repeated infections.

#### (ii) *Methods and experiment procedure*

The methods for producing infective larvae, infection of cats and post mortem recovery of both adult and larval macrofilarial parasites are described in detail in Denham *et al.* (1972*a*) and Suswillo *et al.* (1982).

The infection protocol followed in PI studies consisted of a single inoculation of naive cats with either 100 or 200 infective third-stage larvae (L3), and subsequent serial sacrifice of subsets of animals for the estimation of lymphatic macrofilarial burdens (Denham *et al.* 1972*a*; Suswillo *et al.* 1982). In the more complex RI studies, cats were initially given a primary infection of either 100 or 200 L3, followed, after a delay of between 45 and 200 days (corresponding to the time of early patency of the initial infection), by a regime of repeated infection with 50 L3 at approximately 10-day intervals for up to 1000 days (Denham *et al.* 1972*b*, 1983). As with PI studies, serial post mortem recovery of microfilariae was performed in subsets of cats at various time points after the start of the reinfection regime.

### (b) *Statistical methods*

We need to estimate changes with time in the mean and degree of aggregation of parasitism. Preliminary analyses (Grenfell *et al.*

1991) indicate an aggregated distribution for worm burdens, which is well fitted empirically by a negative binomial distribution. We therefore analyse temporal trends in the mean burden using generalized linear models (GLMs) with negative binomial errors (Wilson & Grenfell 1996), using the S-plus statistical package (Venables & Ripley 1994). This approach assumes (and gives an estimate of) a constant negative binomial shape parameter,  $k$  (inversely measuring the degree of aggregation). We therefore assess changes in aggregation through time by fitting separate models to different epochs.

(c) **Stochastic models**

(i) *Simple analytical models for parasite aggregation in primary infections*

We present a family of models, which are compared with the results of the infection experiments in the next section.

(1) Model A: the homogeneous case. Consider the number of adult parasites ( $M$ ), following a single infection of size  $C$  at time  $t=0$ . Assume, for the moment, that all parasites mature, and that adult parasites have a constant probability of mortality, controlled by a constant per capita death rate,  $m_M$  (i.e. ignoring acquired immunity or differences between hosts). If  $C$  is constant, and denoted  $\phi$  for example, this is a pure death process and  $M$  is binomially distributed, with mean  $m_M = \phi \exp(-m_M t)$  (Anderson & Michel 1977). In fact, the infection dose,  $C$ , for primary infections in the cat model is not constant, but consistent with a Poisson distribution (data from early, i.e. at most a few hours post infection, larval recoveries from a subset of ten cats given single doses of approximately 100 L3: variance:mean=1.37,  $\chi^2=13.67$ , d.f.=9,  $p>0.5$  (Elliott 1977)). In this case,  $M$  is also Poisson, with the same exponential form for  $m_M$ , but where  $\phi$  is now the mean of the distribution of  $C$  (Anderson & Michel 1977). This null model therefore implies *no aggregation* of parasite counts following a primary infection.

(2) Model B: heterogeneities between hosts. The simplest assumption here is to take the above model (with a Poisson-distributed initial infection, with mean  $\langle \phi \rangle$ ), and make the parasite death rate a random variable, which is constant for each host, but different between hosts.

Assume in general that the parasite death rate,  $m_M$  has moment generating function  $G(t)$ , i.e.  $G(t) = E(\exp(-m_M t))$ . For a particular individual with a given  $m_M$ , the parasite load,  $M(t)$ , at time  $t$ , has a Poisson distribution with mean  $\phi \exp(-m_M t)$ . To estimate the degree of aggregation, we require the mean and variance of the worm burden over the whole population. We can obtain these from the following factorial moments. Unconditionally, on  $m_M$  (i.e. over the whole population), if we write  $X^j = X(X-1)(X-2)\dots(X-j+1)$ , then  $E(M^j) = \phi^j$  and  $E(\exp(-jm_M t)) = \phi^j G(jt)$ . So, for example, the mean population parasite load is  $E(M) = \phi G(t)$ , and  $\text{var}(M) = \phi^2 G(2t) + \phi G(t) - [\phi G(t)]^2$ , so that  $M$  is aggregated ( $\text{var}(M) > E(M)$ ) if  $G(2t) > [G(t)]^2$ .

The interpretation of this model is particularly simple if the parasite death rate,  $m_M$  has a gamma distribution with mean  $K/\lambda$  and variance  $K/\lambda^2$ . Here,  $\lambda$  controls the position of the mean and  $K$  is a shape parameter, which gives considerable flexibility to the density function for  $m_M$  (the smaller  $K$  is, for a constant mean, the larger the variance in the death rate will be). For this distribution, the moment generating function is

$$G(t) = (\lambda / (\lambda + t))^K, \tag{1}$$

which leads to the following expressions for the mean, variance and variance/mean ratio of parasite burden

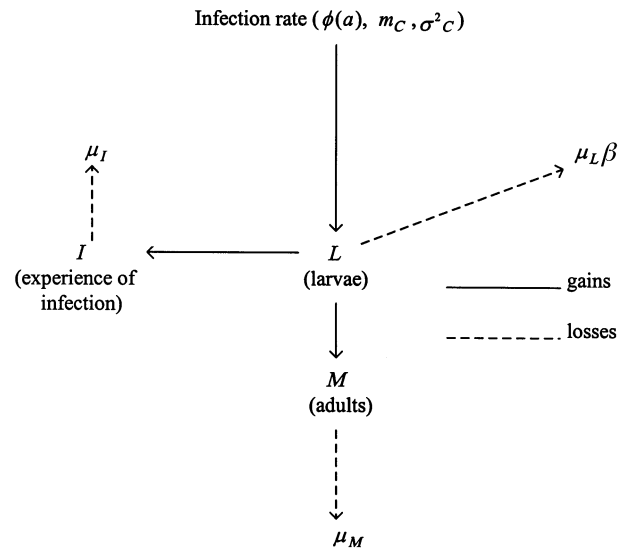


Figure 1. Schematic diagram of the MCE model infection process (see Appendix).

Table 1. *Definitions of model parameters*

loss rates: $\mu_I, \mu_L, \mu_M$	
$1/\mu_I$	duration of immunological memory
$1/\mu_L$	life expectancy of larvae in the host
$1/\mu_M$	life expectancy of adult worms
$\beta$	additional death rate of larvae due to 1 unit of infection experience
infection and developmental rates:	
$\phi(a)$	encounter rate with infective larvae at age, $a$
$m_C, \sigma^2_C$	mean and variance of larvae ingested per encounter
$\gamma_L$	developmental rate of larvae
$v$	rate of increase of immunity level due to larvae

$$E(M(t)) = \phi(\lambda / (\lambda + t))^K, \tag{2}$$

$$\text{var}(M(t)) = \phi^2(\lambda / (\lambda + 2t))^K + E(M(t)) - [E(M(t))]^2. \tag{3}$$

Since the variance/mean ratio is always greater than unity for  $t > 0$ , the population burden is always aggregated.

(ii) *Allowing for repeated infection and immunity: MCEs (model C)*

The above models are very simplistic, in two directions. First, they do not allow for the age structure of the parasite population, especially the differentiation between larval and adult parasites and the process of establishment of larvae (Suswillo *et al.* 1982). Second, the models thus far are *linear*, and do not allow for immunological limitations on present survival of parasites, as a density dependent function of the host's previous experience of infection. Both of these processes are likely to be important in filariasis (Denham & Fletcher 1987; Wenk 1991; Bundy *et al.* 1991; Ottesen 1992)—particularly in the case of repeated infections (Denham *et al.* 1972*b*, 1983, 1992; Denham & Fletcher 1987; Grenfell *et al.* 1991). Though the above linear models could in principle be extended to allow for parasite age structure, nonlinearities, such as acquired immunity, make the forward equations for the second moments of the parasite distribution dependent on the third, etc., so that equations for the moments cannot be written down in closed form (Isham 1995; Grenfell *et al.* 1995*a*).

The MCE approach allows for this by modelling the third moments using a normal approximation (Whittle 1957; Isham 1991). Full details are given by Isham (1991, 1995) and Grenfell *et al.* (1995*a,b*); here we describe the structure and biological assumptions of the model. Figure 1 and table 1 summarize the model's biological assumptions and parameters.

#### *The infection process*

In order to allow for future models including variation due to vector biting, variability in infection rate is modelled explicitly by using a compound Poisson process. Thus, we assume that, for any individual host, encounters with parasite transmission stages occur in an inhomogeneous Poisson process with rate  $\phi(a)$ , depending on the age,  $a$ , of the individual. During an encounter, the number of parasites input,  $C$ , is a random variable with mean  $m_C$  and variance  $\sigma_C^2$ . In this paper, we take  $m_C=1$  and  $\sigma_C^2=0$ , so that the infection rate reduces to an ordinary (inhomogeneous) Poisson process.

The model tracks infection variability through larval ( $L$ ) and adult ( $M$ ) parasite stages. Additional variability due to differences between hosts can then be modelled by replicating the model's equations with varying parameters (see below). The constant background per capita death rates of larvae and adults are denoted by  $\mu_L$  and  $\mu_M$  per unit time, respectively.

#### *Nonlinear effects: immunity and parasite-induced host mortality*

Immunity to helminth infections is generally considered to accumulate with the host's previous experience of larval intake (Anderson & May 1991; Maizels *et al.* 1993; Woolhouse 1992). Here, we make the mathematically simplest assumption that previous experience of infection ( $I$ ) accumulates with the larval burden ( $L$ )—at rate  $v$ , and decays at rate  $\mu_I$  (so that  $1/\mu_I$  is the average 'memory' of previous infection (Grenfell *et al.* 1995*a*)). Since immunity appears to develop progressively in the cat model for filariasis (Denham *et al.* 1972*b*, 1983), we take  $\mu_L=0$  (i.e. no fading of immune memory)—the following results are not sensitive to this assumption. Previous experience of infection ( $I$ ) is assumed to increase the mortality of larvae by a rate  $\beta$ . Since we deal here with chronically infected cats, which do not throw off adult infection, we do not allow for any effect of immunity on adult parasite survival (Denham *et al.* 1972*b*, 1983; Grenfell *et al.* 1991). This effect (as well as parasite-induced host mortality and *concomitant immunity* accumulating from the adult burden) can easily be included (Grenfell *et al.* 1995*b*).

#### *Parasite variables*

The model tracks parasite abundance and average immunological experience as a function of host age ( $a$ ), in terms of the first moment (mean). This is denoted by  $m_A(a)$  where  $A=I, L, M$ , for the respective variables. The variability of the system is represented by the second moments, for example  $\sigma_L^2(a)$  is the variance of larval counts and  $\sigma_{IL}(a)$  is the covariance of immunity and larval burden.

The Appendix sets out a series of ordinary differential equations to describe the dynamics of these variables as a function of host age. We then assess parasite aggregation by the moment estimate of the negative binomial parameter,  $k$ . For example,  $k$  for adult parasites is given by

$$k_M(a) = \frac{m_M(a)^2}{\sigma_M^2(a) - m_M(a)}. \quad (4)$$

The covariances allow us to assess correlations between parasite variables (Grenfell *et al.* 1995*b*).

### 3. RESULTS AND DISCUSSION

#### (a) *Primary infections*

##### (i) *Observed temporal trends*

Figure 2 shows the proportion of macrofilariae recovered at different times after initial infections with 100 or 200 larvae. It indicates a relatively noisy decline in counts, with a relatively large initial drop up to day 50, and no obvious difference in the proportion recovered as a function of infection dose. This is confirmed using results from GLMs, which are also summarized in the figure. Specifically, given the count data, we used a log link between observations and time as the linear predictor (Venables & Ripley 1994), and found a significant effect of time after day 40 (slope =  $-0.00147 \text{ d}^{-1}$ ,  $p=0.0037$ ), with no evidence of a difference in slopes between the two infection levels. Given the log link, this indicates an exponential decay in counts after day 40 (figure 2), with an estimated average adult parasite life expectancy of  $1/\text{slope}=1.86$  years, which accords with previous estimates for this model (Grenfell *et al.* 1991; Denham *et al.* 1992). Counts before day 40 are higher than predicted by the regression line, indicating that about 65% of the initial larval population (or 30% of the overall larval dose (figure 2)), establish in the cat lymphatics by day 40 (Suswillo *et al.* 1982). The similar slope (and therefore survivorship) for the two treatments indicates that there is no evidence, on the basis of these data, for density-dependent immunological constraints on parasite survival following a primary infection.

##### (ii) *Patterns of aggregation*

The above analysis indicated an overall negative binomial  $k$  for the primary data of  $k=3.29$  (s.e.=0.4). However, we are also interested in tracking observed changes in aggregation over the course of the infection. We do this by a simple partitioning of the data into blocks of roughly equal sample size (see the mean burden for each block in figure 3*a*); the choice of blocking does not affect the qualitative results. Rather than estimate  $k$  directly for each of these blocks (which would confound variability with the temporal trend), we use the GLM to calculate  $k$ , allowing for the observed decay in worm burden with time. The resulting  $k$  estimates are shown in figure 3*c,d*. Essentially,  $k$  increases roughly exponentially with the mean (figure 3*d*), reflecting a decline in the two parameters with time (figure 3*a,c*). As mentioned previously, the initial variance/mean ratio of larval dose does not differ significantly from a Poisson distribution, corresponding to a large value of  $k$ . The estimated  $k$  therefore decreases abruptly from this level soon after the start of the experiment.

##### (iii) *Analytical models: models A and B*

The GLM analysis summarized in figure 3 indicates that the data from the primary infection experiments are significantly aggregated. This immediately rules out the simple null model (*A*), in which a Poisson-distributed initial infection suffers a constant initial death rate, leading to a Poisson distribution for the adult burden.

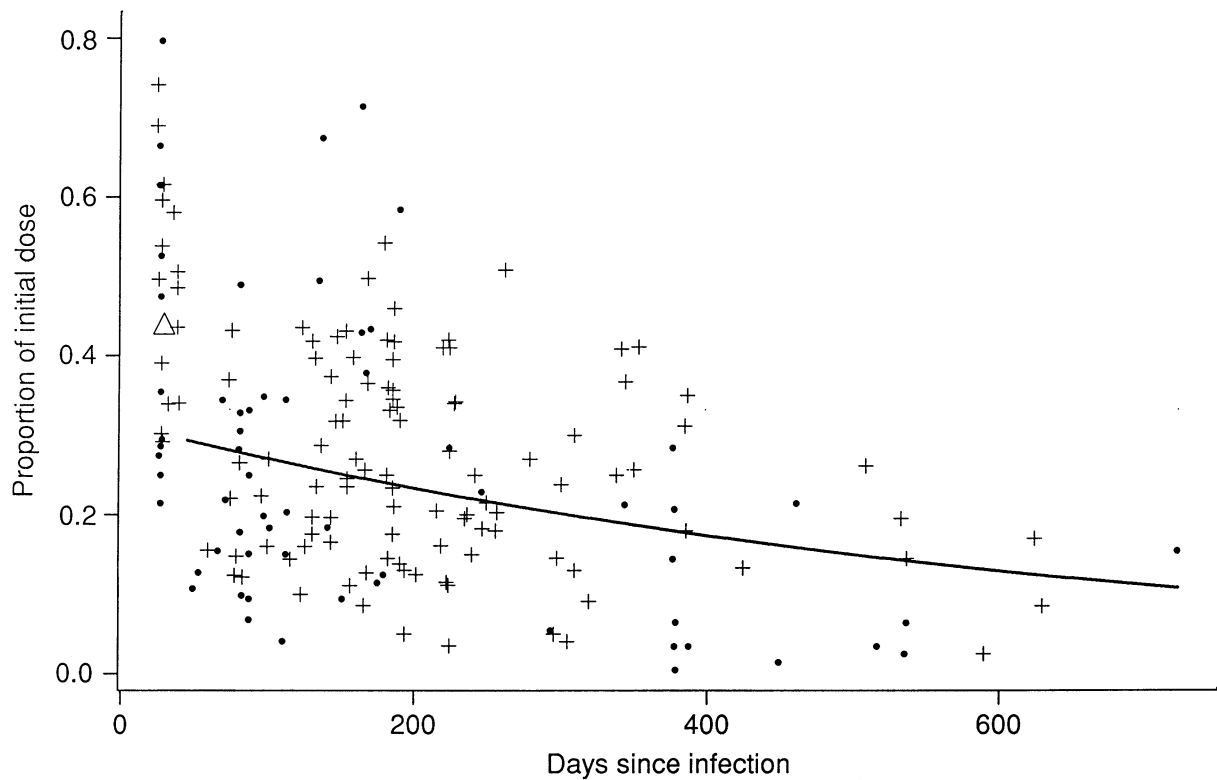


Figure 2. Macrofilarial counts from the primary infection experiments. Each point represents the recovered worm count as a proportion of initial infection dose in hosts dissected at the specified time (dots and crosses, 100 and 200 average infection dose, respectively). The curve is the fit to post day 45 data of the GLM described in the text. The triangle shows the fit of a null GLM (intercept or mean only) to the earlier data.

Figure 3e–g explores the aggregation pattern generated by model B, in which the adult death rate is assumed to be gamma-distributed, with different degrees of variability (measured inversely by the dispersion parameter,  $K=0.1, 1, 10$ ). For large  $K$ , the decay with time in mean parasite burden (figure 3e) is very similar to the deterministic case, also shown on the figure. However, as  $K$  decreases, the population parasite survival curve reflects a lower average death rate. This is because the distribution for the parasite death rate,  $m_M$  is skewed towards low values, which generate a higher survivorship. Moment estimates of the negative binomial  $K$  for the population also decay with time (figure 3f), as the—initially identical—Poisson distributions of infection in different hosts diverge due to the heterogeneities in parasite death rate. Because of this pattern,  $k$  is positively associated with the population mean burden (figure 3g), increasing exponentially with the mean for low burdens, then hyperbolically towards infinity, as the distributions in individual hosts converge towards the same Poisson distribution. Not surprisingly, as  $K$  declines (and therefore the variability of the distribution of death rates increases), the aggregation of the population increases, and therefore the negative binomial  $k$  in figure 3g is lower for a given mean burden.

Figure 3g also shows the observed  $k$  versus mean relationship for the primary infections. Though model B captures the observed qualitative increase in  $k$ , it shows a much steeper slope in  $k$  than the observed data. In fact, this simple model is hard to compare in detail with the data, since it does not include a realistic measurement of

parasite age structure (and therefore the initial establishment of larvae). We can correct for this by using the more biologically detailed MCE model described above.

(iv) *An MCE model for primary infections: model C*

The GLM analysis gives us the average death rate of adult parasites,  $\mu_M=0.00147 \text{ d}^{-1}$ . Given an average larval duration of 25 days (Suswillo *et al.* 1982), and assuming no acquired immunity for primary infections (so that  $\beta=0$ ), we only need to estimate the larval death rate  $\mu_L$ . Figure 4a shows a numerical solution of the moment equations, which matches the exponential decay in worm burden estimated from the GLM. This requires a high larval death rate of  $\mu_L=0.085 \text{ d}^{-1}$ , reflecting the initial loss of larvae (Suswillo *et al.* 1982), to 30% by day 40. In fact, the model overestimates the speed of this decline (figure 4a), probably because we have not allowed completely for time delays in larval development.

To model differences in parasite death rate between hosts, we simply replicate solutions with varying death rates, then calculate overall population means and variances. In principle, we could add variability to either or both the larval and adult death rates. Figure 4b,c shows the effects of introducing gamma-distributed variations in  $\mu_L$  and  $\mu_M$ , respectively (keeping the other death rate constant). Clearly, though both cases could qualitatively account for the variability in worm burdens at the end of the experiment, adult death rate variability alone does not account for the large initial variations in worm burden observed during the experiment. It looks, therefore, as

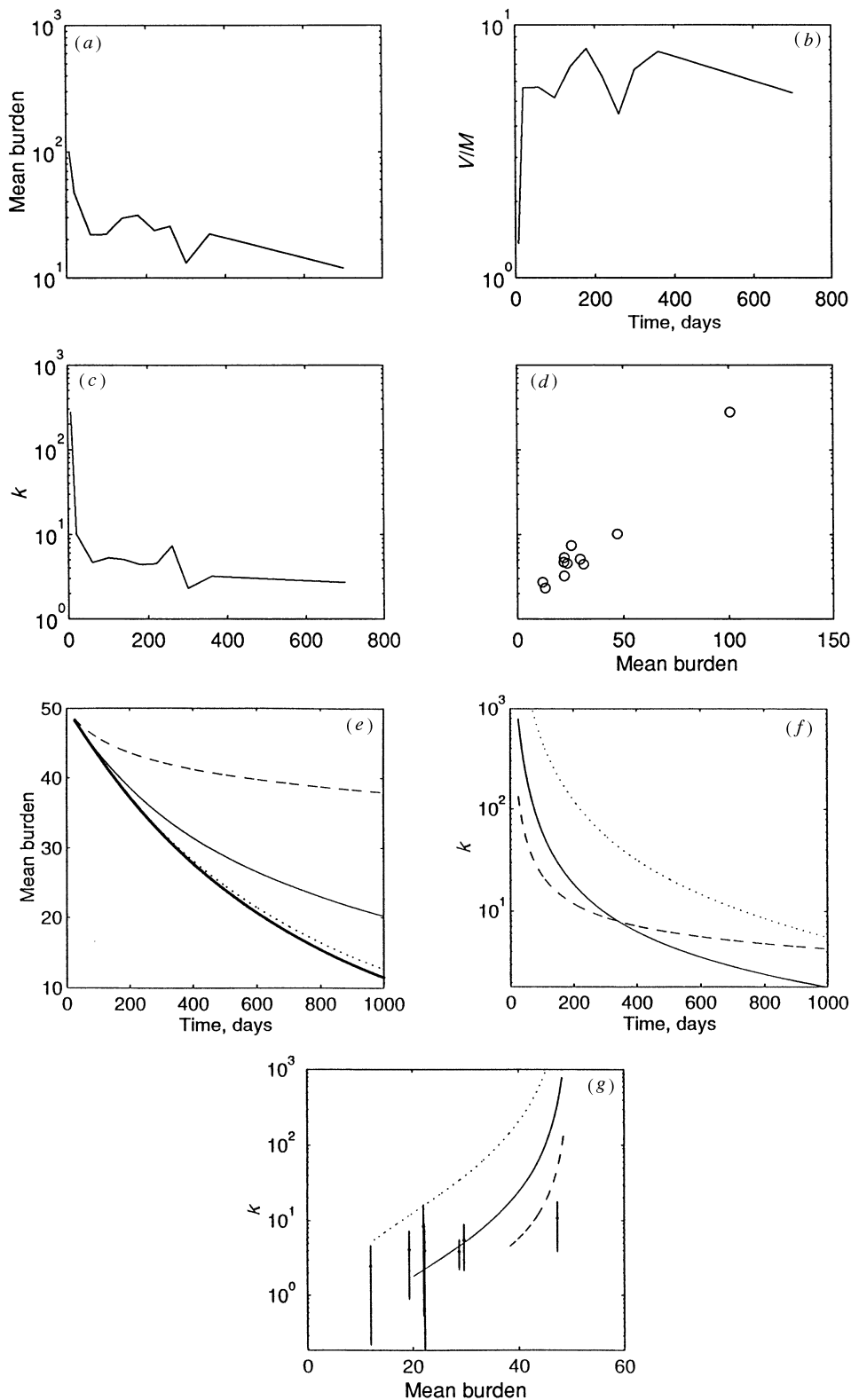


Figure 3. (a)–(d) Observed pattern of aggregation for the primary infections. The series was split at time points,  $t=40, 80, 120, 160, 200, 240, 280, 320$  and  $400$ , and the data for both infection levels were pooled after dividing the 200 infection level counts by 2. (a) Mean burden; (b) variance to mean ratio; (c) moment estimate of the negative binomial parameter  $k$  (calculated via the GLM fits as described in the text) against time; (d)  $k$  against the mean count. (e)–(g) Equivalent plots for model B (gamma-distributed adult parasite death rates), as described in the text. Dotted, solid and dashed lines refer, respectively, to values of  $K=10, 1, 0.1$ , for the gamma-distributed dispersion parameter. We start the model at a worm burden of 50, for  $t=0$ , to allow for the initial drop in the establishment in the primary infections. (e) Mean burdens (the thick line is the deterministic model, with the mean parasite death rate for the gamma distribution); (f)  $k$  versus time; (g)  $k$  versus mean burden. The points and bars in (g) denote the moment estimates of  $k$  from the observed data and the corresponding s.e.s. of the estimates, respectively, at each mean burden.

though we require at least some variation in  $\mu_L$  to model the time course of parasite variability.

Figure 4*d* shows a plot of the estimated negative binomial  $k$  for the overall population against population mean, corresponding to the simulations of figure 4*b*. As shown, this more biologically realistic model is a much better overall mimic of the observed pattern of aggregation for primary infections. One discrepancy between model and data is that the former shows a plateau in  $k$  as the mean declines, whereas  $k$  continues to fall in the observed series. As shown in figure 4*d* by a simulation superimposing some variation in  $\mu_M$ , this may be because we also require some variation in adult death rate, to keep the variability increasing.

**(b) Repeated infections**

(i) *Observed temporal trends and variability*

Figure 5*a* displays adult worm counts for the two sets of repeated infection experiments (RI100 and RI200, with initial mean doses of 100 and 200 larvae, respectively). Both series show initial variability in counts with (at least for RI200) signs of a subsequent decline. Figure 5*a* also superimposes the fitted curve and prediction confidence limits for the primary infection model. We return to this comparison after examining the basic RI patterns. Because RI200 is a much larger data set, we concentrate on this case first.

Figure 5*b* shows the best fit GLM for the RI200 data. Because of the large reduction in variability about 250 days post initial infection, we considered the data before and after this period separately. Before  $t=250$  d, the data are relatively variable ( $k=3$ ), with no evidence of a trend with time. After  $t=250$  d, there is a significant decline in counts with time (slope =  $-0.0024 \text{ d}^{-1}$ ,  $p < 0.00001$ ), which are much less variable ( $k=62$ ). A similar pattern of declining variability with time is apparent in the RI100 data ( $k=2.7$ , before  $t=400$ ;  $k=7$ , for  $t > 400$ ), though there is no significant decline with time in these data (figure 5*a*).

(ii) *Patterns of acquired immunity*

As reviewed above, cats infected with *B. pahangi* show a strong immunity against incoming larvae from subsequent repeat infections (Denham *et al.* 1972*b*, 1983). This is reflected in figure 5*a*, where the prediction confidence limits for the primary infection bracket the later data for the repeat infection. In other words, by the end of the RI200 experiment, we can account for the adult worm burden simply by the survivors from the initial primary infection, even though several thousand larvae have been injected over the intervening period.

We can explore this effect with the MCE model derived for primary infections (figure 4*a*), at a range of levels of  $\beta$ , the additional death rate of larvae due to immunity. As shown in figure 6*a*, the model for repeat infection (RI200) without immunity ( $\beta=0$ ) greatly overestimates the observed burdens, whereas an immunity level around  $\beta=0.005$ , captures the level of reduction in larval survival necessary to mimic observed adult worm burdens by the end of the experiment. The corresponding mean level of previous infection experience on which immunity acts is shown in figure 6*b*. Immunity to larval establishment is thought to be controlled in part by IgE levels (Baldwin *et al.* 1993)—these are superimposed on the model immunity

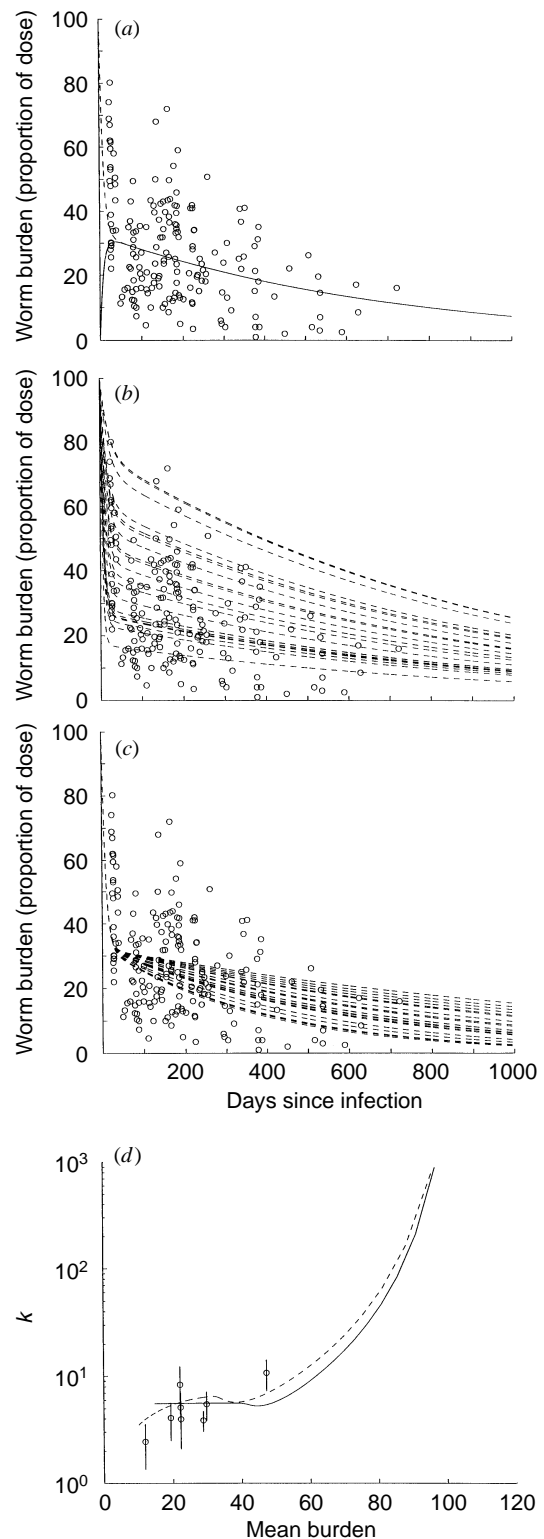


Figure 4. (a) Fit of the MCE model to primary infection data. As described in the text, the model was simulated by standard numerical methods; solid line, adult burden; dashed line, total burden. (b) A set of 20 equivalent simulations, with random (gamma-distributed  $K=3$ ) larval death rates; (c) 20 simulations with gamma-distributed adult death rates ( $k=3$ ); (d) solid line, moment estimate of adult parasite negative binomial  $k$  for the population defined by the simulations in (b);  $k$  was calculated from the overall variance of the simulations and is plotted against the mean burden. Dashed line, similar estimates from simulations with gamma-distributed variation on adult worm death rate ( $K=10$ ). The observed  $k$  estimates (figure 3*g*) are also shown.

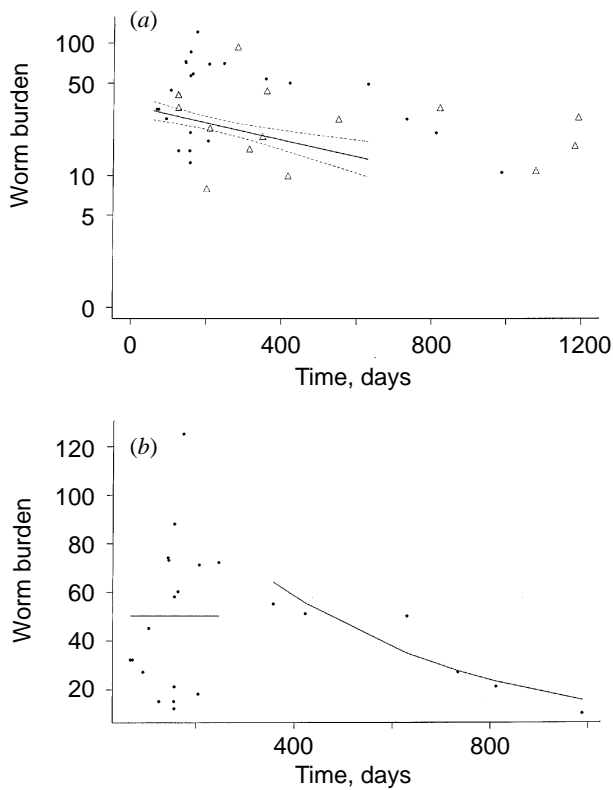


Figure 5. (a) Results of the repeated infection experiments (triangles, RI100; dots, RI200). The lines and dotted 95% prediction error bars are from the GLM fit to the primary infection data with initial dose of 200 larvae. (b) GLM fits to the RI200 data, as described in the text.

level in figure 6*b*; though the model captures the qualitative IgE pattern of a rise to a plateau, the latter rise much more slowly, apparently after a time delay. If IgE is a measure of the immunity level, this indicates that our simple model is producing too rapid a rise in immunity. However, in order to match the dynamics of primary and repeated infections, we do seem to require earlier constraints on the establishment of repeat infections that the IgE rise implies.

### (iii) Modelling variability in the repeat infections

The model solution in figure 6*a* (which generates an approximately Poisson-distributed adult burden) does not capture the observed variability in parasite counts up to day 250. Figure 6*c* explores the effect on this picture of heterogeneity between hosts in the larval death rate (as explored in figure 4*b* for the primary infections). Essentially, this heterogeneity in establishment of larvae generates a variability in the early part of the series, which then declines with time. This result is shown more systematically in figure 7*a–c*, via changes with time in the population mean and negative binomial  $k$  estimate, for the solutions in figure 6*c*.  $k$  falls very rapidly at the start of the experiment as heterogeneities in larval death rate move the population worm distribution away from a Poisson (figure 7*b*), then has a negative relationship with the mean, progressively increasing as the mean declines (figure 7*c*). This progressive decrease in parasite aggregation over most of the course of infection qualitatively

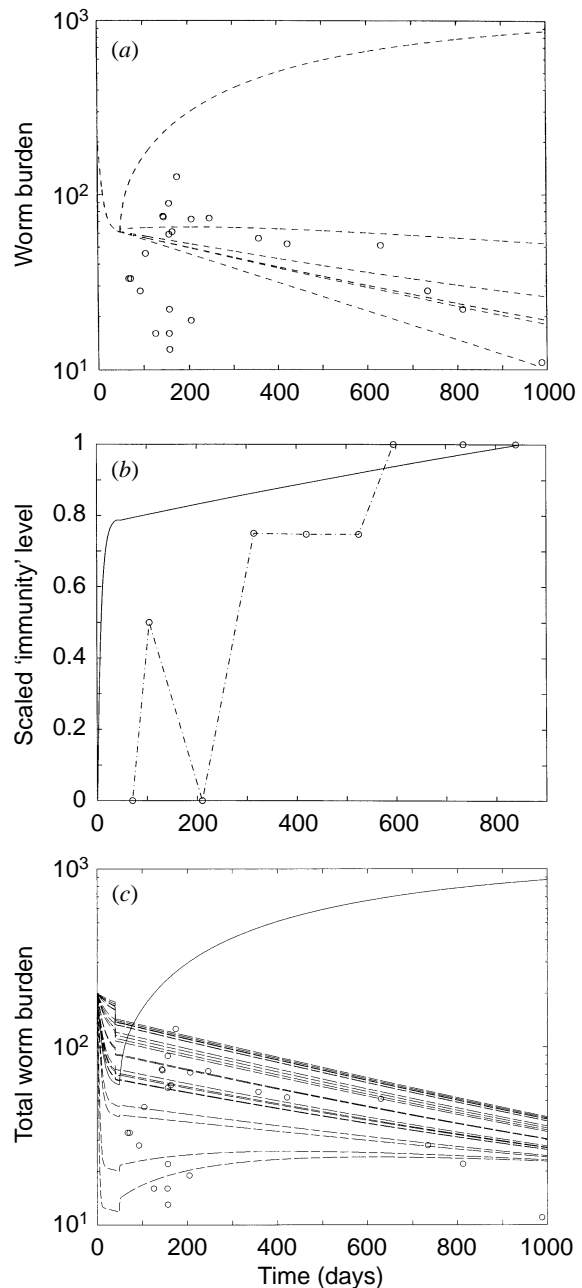


Figure 6. (a) MCE model simulations (as described in the text) compared to the RI200 worm counts. The dotted curves span a range of immunological limitations imposed on cohorts of larvae after the primary infection. Top curve, no immunity ( $\beta=0$ ); curves moving down the page refer to increasing levels of immunity ( $\beta=0.001, 0.005, 0.015, 0.02$ , and  $1$ , per day per unit level of immunity). (b) Scaled (on 0,1) mean level of previous experience of infection ( $m_L$  in the Appendix) for the  $\beta=0.005$  simulation (solid line), along with observed IgE counts (scaled on 0,1) taken during the RI200 experiments (open circles joined by dashed line). The IgE data are as documented in the text. (c) 20 simulations of the RI200 experiment ( $\beta=0.005$ ) with gamma-distributed larval death rate ( $K=1$ ).

mirrors what we observe in RI100 and 200—though this result should be viewed cautiously, since the empirical data become very sparse by the end of the experiments.

In the model, this effect of decreasing aggregation reflects the impact of a common level of immuno-

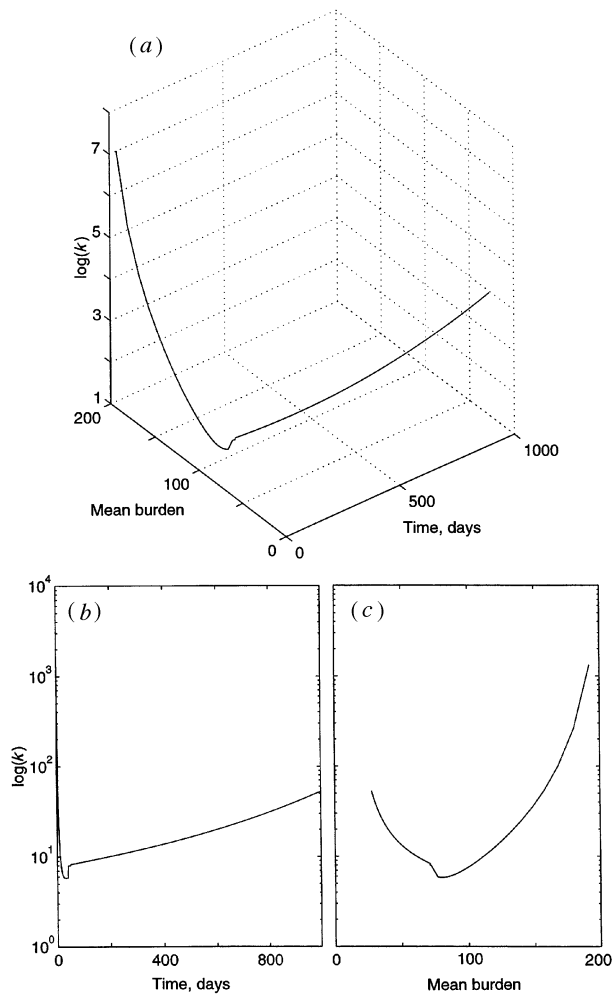


Figure 7. Analysis of parasite population aggregation from the simulations shown in figure 6c. The population mean and negative binomial  $k$  are plotted against time in various combinations.

competence between cats. Essentially, this nonlinearity acts in the model as a ‘filter’, gradually removing the variability generated by heterogeneities in larval mortality as immunity builds up with time. This implies that there may be some degree of homogeneity in immune mechanisms in hosts infected with filariasis. In particular, further numerical solutions of the model equations (not documented here) show that heterogeneities in immunity (modelled by variations in  $\beta$ ) can cause an increase in variability with time of infection, since hosts then have a different asymptotic death rate of parasites. This contrasting picture is what we see, from both empirical data and models, for gastrointestinal nematode parasites of sheep (Grenfell *et al.* 1995a).

In fact, other data from the cat model show considerable heterogeneity in immune responses between this and other groups of cats (Denham *et al.* 1992), so that we will need to refine the model to assess the overall implications of the system for heterogeneity. It is interesting, however, that the removal of parasite variability with host age, documented above, is also seen in microfilarial counts

from human populations (Grenfell *et al.* 1990; Das *et al.* 1990).

#### 4. CONCLUSION

The main result of this analysis of variability in the cat model for lymphatic filariasis is that aggregation is constant or increases following primary infection, whereas it decreases under conditions of repeated infection. We use a hierarchy of stochastic models to account for this pattern in terms of the powerful immune response which hosts mount against repeat infections. The primary infection results are consistent with heterogeneities in the survival of parasite infections between hosts. Though other explanations may be possible, further work (Grenfell *et al.* 1991) does indicate significant heterogeneities between cats in microfilarial counts following primary infection. The models then indicate that the reduction with time (essentially host age) in parasite variability in the repeat infections is consistent with the ‘filtering’ effects of similar immune responses. More generally, this homogenizing effect of density dependence is seen in a number of host–parasite systems (Anderson & Gordon 1982; Pacala & Dobson 1988), though in many others, the degree of variability increases in older animals, as worm burdens decline (Grenfell *et al.* 1995b).

The homogeneity of immune responses assumed here may be reasonable for the relatively immunologically similar group of ‘chronically’ infected hosts analysed in this paper—in future models, we shall need to extend the analysis to the groups of cats with more spectacularly effective responses to infection (Grenfell *et al.* 1991; Denham *et al.* 1992). In addition, although our assumption (that host heterogeneity in response is manifested only in variations in larval survival rate) captures the qualitative pattern of a decline in parasite variability with time during the repeat infections, it is apparent (figure 6c), that this is only a relatively crude mimic of the observed temporal pattern of infection. Future progress here may require models to represent more explicitly the dynamics of immunity—for example, reflecting different hypotheses about the roles of IgE, IgG4 and other cells and molecules (Maizels *et al.* 1995; Mahanty & Nutman 1995). The first step is probably to include the dynamics of microfilariae as well as adult worms (Grenfell *et al.* 1991), since microfilariae seem to have an important role in modulating anti-filarial immunity (Ottesen 1992; Maizels *et al.* 1995; Mahanty & Nutman 1995).

The data used in this analysis would have been without value unless collected with great care. We thank F. Guy, T. Ponnudurai, R. Rogers, R. Suswillo, P. McGreevy, P. Oothuman, C. Fletcher, D. Birch, C. Baldwin, and F. de Medeiros. E.M., B.T.G. and D.A.P.B. gratefully acknowledge the financial support of the Wellcome Trust. B.T.G. and V.S.I. acknowledge the support of BBSRC and EPSRC in facilitating this work.

#### APPENDIX 1

The model described in the text is defined by the following equations for the first two moments of the parasite distribution. A full derivation of the model is given by Grenfell *et al.* (1995a,b).

$$\begin{aligned}
\frac{dm_I}{da} &= \nu m_L - \mu_I m_I; \\
\frac{dm_L}{da} &= \phi(a)m_C - \beta\sigma_{IL} - (\mu_L + \gamma_L + \beta m_I)m_L; \\
\frac{dm_M}{da} &= \gamma_L m_L - \mu_M m_M; \\
\frac{d\sigma_I^2}{da} &= \nu m_L + \mu_I m_I + 2\nu\sigma_{IL} - 2\mu_I\sigma_I^2; \\
\frac{d\sigma_L^2}{da} &= \phi(a)(\sigma_C^2 + m_C^2) + (\mu_L + \gamma_L + \beta m_I)m_L - \\
&\quad \beta(2m_L - 1)\sigma_{IL} - 2(\mu_L + \gamma_L + \beta m_I)\sigma_L^2; \\
\frac{d\sigma_M^2}{da} &= \gamma_L m_L + \mu_M m_M + 2\gamma_L\sigma_{ML} - 2\mu_M\sigma_M^2; \\
\frac{d\sigma_{IL}}{da} &= \nu\sigma_L^2 - \beta m_L\sigma_I^2 - (\mu_I + \mu_L + \gamma_L + \beta m_I)\sigma_{IL}; \\
\frac{d\sigma_{IM}}{da} &= \nu\sigma_{LM} + \gamma_L\sigma_{IL} - (\mu_I + \mu_M)\sigma_{IM}; \\
\frac{d\sigma_{LM}}{da} &= \gamma_L(\sigma_L^2 - m_L) - \beta m_L\sigma_{IM} - (\mu_L + \gamma_L + \\
&\quad \beta m_I + \mu_M)\sigma_{LM}.
\end{aligned} \tag{A1}$$

## REFERENCES

- Amaral, F., Dreyer, G., Figueredo-Silva, J., Noroes, J., Cavalcanti, A., Sarnico, S. C., Santos, A. & Coutinho, A. 1994 Adult worms detected by ultrasonography in human bancroftian filariasis. *Am. J. Trop. Med. Hyg.* **50**, 753–757.
- Anderson, R. M. & Gordon, D. 1982 Processes influencing the distribution of parasite numbers within host populations with special emphasis on parasite-induced host mortalities. *Parasitology* **85**, 373–378.
- Anderson, R. M. & May, R. M. 1991 *Infectious diseases of humans: dynamics and control*. Oxford University Press.
- Anderson, R. M. & Michel, J. F. 1977 Density dependent survival in populations of *Ostertagia ostertagi*. *Int. J. Parasitol.* **7**, 321–329.
- Baldwin, C. I., de Medeiros, F. & Denham, D. A. 1993 IgE responses in cats infected with *Brugia pahangi*. *Para. Immunol.* **15**, 291–296.
- Berding, C., Keymer, A. E., Murray, J. D. & Slater, A. F. G. 1986 The population dynamics of acquired immunity to helminth infection. *J. Theor. Biol.* **122**, 459–471.
- Bundy, D. A. P., Grenfell, B. T. & Rajagopalan, P. K. 1991 Immunoepidemiology of lymphatic filariasis: the relationship between infection and disease. *Immunoparasitol. Today* A71–A75.
- Croll, N. A. 1983 Human behaviour, parasites, and infectious diseases. In *Human ecology and infectious diseases* (ed. N. A. Croll & J. H. Cross), pp. 1–20. London: Academic Press.
- Crombie, J. A. & Anderson, R. M. 1985 Population dynamics of *Schistosoma mansoni* in mice repeatedly exposed to infection. *Nature* **315**, 491–493.
- Das, P. K., Manoharan, A., Srividya, A., Grenfell, B. T., Bundy, D. A. P. & Vanamail, P. 1990 Frequency distribution of *Wuchereria bancrofti* microfilariae in human populations and its relationships with age and sex. *Parasitology* **101**, 429–434.
- Denham, D. A. & Fletcher, C. 1987 The cat infected with *Brugia pahangi* as a model of human filariasis. *CIBA Foundation Symp.* **127**, 225–235.
- Denham, D. A., McGreevy, P. B., Suswillo, R. R. & Rogers, R. 1983 The resistance to re-infection of cats repeatedly inoculated with infective larvae of *Brugia pahangi*. *Parasitology* **86**, 11–18.
- Denham, D. A., Ponnudurai, T., Nelson, G. S., Guy, F. & Rogers, R. 1972a Studies with *Brugia pahangi*. I. Parasitological observations on primary infections of cats (*Felis catus*). *Int. J. Parasitol.* **2**, 239–247.
- Denham, D. A., Ponnudurai, T., Nelson, G. S., Rogers, R. & Guy, F. 1972b Studies with *Brugia pahangi*. II. The effect of repeated infection on parasite levels in cats. *Int. J. Parasitol.* **2**, 401–407.
- Denham, D. A., Medeiros, F., Baldwin, C., Kumar, H., Midwinter, I. C. T., Birch, D. W. & Smail, A. 1992 Repeated infection of cats with *Brugia pahangi*: parasitological observations. *Parasitology* **104**, 415–420.
- Dietz, K. 1982 Overall population patterns in the transmission cycle of infectious agents. In *Population biology of infectious diseases* (ed. R. M. Anderson & R. M. May), pp. 87–102. Berlin: Springer.
- Dreyer, G., Amaral, F., Noroes, J. & Medeiros, Z. 1994 Ultrasonographic evidence for stability of adult worm location in bancroftian filariasis. *Trans. R. Soc. Trop. Med. Hyg.* **88**, 558.
- Elliott, J. M. 1977 *Statistical analysis of samples of benthic invertebrates*, 2nd edn. Ambleside: Freshwater Biological Association.
- Grenfell, B. T., Dietz, K. & Roberts, M. G. 1995a Modelling the immuno-epidemiology of macroparasites in naturally fluctuating host populations. In *Ecology of infectious diseases in natural populations* (ed. B. T. Grenfell & A. Dobson), pp. 362–383. Cambridge University Press.
- Grenfell, B. T., Michael, E. & Denham, D. A. 1991 A model for the dynamics of human lymphatic filariasis. *Parasitol. Today* **7**, 318–323.
- Grenfell, B. T., Smith, G. & Anderson, R. M. 1987a A mathematical model of the population biology of *Ostertagia ostertagi* in calves and yearlings. *Parasitology* **95**, 389–406.
- Grenfell, B. T., Smith, G. & Anderson, R. M. 1987b The regulation of *Ostertagia ostertagi* populations in calves: the effect of past and current experience of infection on proportional establishment and parasite survival. *Parasitology* **95**, 363–372.
- Grenfell, B. T., Das, P. K., Rajagopalan, P. K. & Bundy, D. A. P. 1990 Frequency distribution of lymphatic filariasis microfilariae in human populations: population processes and statistical estimation. *Parasitology* **101**, 417–427.
- Grenfell, B. T., Wilson, K., Isham, V. S., Boyd, H. E. G. & Dietz, K. 1995b Modelling patterns of parasite aggregation in natural populations: trichostrongylid nematode–ruminant interactions as a case study. *Parasitology* **111**, S135–S151.
- Hadeler, K. P. & Dietz, K. 1983 Nonlinear hyperbolic partial differential equations for the dynamics of parasitic populations. *Comput. Math. Applic.* **3**, 415–430.
- Isham, V. 1991 Assessing the variability of stochastic epidemics. *Math. Biosci.* **107**, 209–224.
- Isham, V. 1995 Stochastic models of host–macroparasite interaction. *Ann. Appl. Prob.* **5**, 720–740.
- Kretzschmar, M. 1989 Persistent solutions in a model for parasitic infections. *J. Math. Biol.* **27**, 549–573.
- Kretzschmar, M. & Adler, F. 1993 Aggregated distributions in models for patchy populations. *Theor. Popul. Biol.* **43**, 1–30.
- Maizels, R. M., Bundy, D. A. P., Selkirk, M. E., Smith, D. F. & Anderson, R. M. 1993 Immunological modulation and evasion by helminth parasites in human populations. *Nature* **365**, 797–805.
- Maizels, R. M., Sartono, E., Kurniawan, A., Partono, F., Selkirk, M. E. & Yazdanbakhsh, M. 1995 T-cell activation and the balance of antibody isotypes in human lymphatic filariasis. *Parasitol. Today* **11**, 50–56.
- Mahanty, S. & Nutman, T. 1995 Immunoregulation in human lymphatic filariasis: the role of interleukin 10. *Parasite Immunol.* **17**, 385–392.

- Medley, G. F. 1992 Which came first in host–parasite systems: density dependence or parasite distribution? *Parasitol. Today* **8**, 321–322.
- Michael, E., Bundy, D. A. P. & Grenfell, B. T. 1996 Re-assessing the global prevalence and distribution of lymphatic filariasis. *Parasitology* **112**, 409–428.
- More, S. J. & Copeman, D. B. 1990 A highly specific and sensitive monoclonal antibody-based ELISA for the detection of circulating antigen in bancroftian filariasis. *Trop. Med. Parasitol.* **41**, 403–406.
- Ottesen, E. A. 1992 Infection and disease in lymphatic filariasis—an immunological perspective. *Parasitology* **104**, S71–S79.
- Ottesen, E. A. 1994 The human filariasis: new understandings, new therapeutic strategies. *Curr. Opin. Infect. Dis.* **7**, 550–558.
- Ottesen, E. A. & Ramachandran, C. P. 1995 Lymphatic filariasis infection and disease: control strategies. *Parasitol. Today* **11**, 129–131.
- Pacala, S. W. & Dobson, A. P. 1988 The relation between the number of parasites/host and host age: population dynamic causes and maximum likelihood estimation. *Parasitology* **96**, 197–210.
- Park, C. B. 1988 Microfilaria density distribution in the human population and its infectivity index for the mosquito population. *Parasitology* **96**, 265–271.
- Pielou, E. C. 1977 *Mathematical ecology*. New York: Wiley.
- Plaisier, A. P., van Oortmarssen, G. J., Hebbema, J. D. F., Remme, J. & Alley, E. S. 1990 ONCHOSIM, a simulation model for the transmission and control of onchocerciasis. *Comp. Meth. Program. Biomed.* **31**, 43–56.
- Quinnell, R. J. & Keymer, A. E. 1990 Acquired immunity and epidemiology. In *Parasites, immunity and pathology: the consequences of parasitic infections in mammals* (ed. J. M. Behnke), pp. 317–343. London: Taylor & Francis.
- Remme, H., Alley, S. & Plaisier, A. 1995 Estimation and prediction in tropical disease control: the example of onchocerciasis. In *Epidemic models: their structure and relation to data* (ed. D. Mollison), pp. 372–393.
- Scott, M. E. 1987 Temporal changes in aggregation: a laboratory study. *Parasitology* **94**, 583–595.
- Shaw, D. J. & Dobson, A. P. 1996 Patterns of macroparasite abundance and aggregation in wildlife populations: a quantitative review. *Parasitology* **111**, S.
- Suswillo, R. R., Denham, D. A. & McGreevy, P. B. 1982 The number and distribution of *Brugia pahangi* in cats at different times after a primary infection. *Acta Tropica* **39**, 151–156.
- Turner, P., Copeman, B., Gerisi, D. & Speare, R. 1992 A comparison of the Og4C3 antigen capture ELISA, the Knott test, an IgG4 assay and clinical signs in the diagnosis of bancroftian filariasis. *Trop. Med. Parasitol.* **44**, 45–48.
- Venables, W. N. & Ripley, B. D. 1994 *Modern applied statistics with S-plus*. New York: Springer.
- Wasson, D. L., Dick, T. A., Arnasson, N., Strickland, D. & Grundmann, A. W. 1986 Host genetics: a key factor in regulating the distribution of parasites in natural host populations. *J. Parasitol.* **72**, 334–337.
- Weil, G. J. 1990 Parasite antigenemia in lymphatic filariasis. *Expl Parasitol.* **71**, 353–356.
- Wenk, P. 1991 The vector host link in filariasis. *Ann. Trop. Med. Parasitol.* **85**, 139–147.
- Whittle, P. 1957 On the use of the normal approximation in the treatment of stochastic processes. *J. R. Statist. Soc. B* **19**, 268–281.
- Woolhouse, M. E. J. 1992 A theoretical framework for the immunoepidemiology of helminth infection. *Parasite Immunol.* **14**, 563–578.
- WHO 1987 WHO Expert Committee on onchocerciasis: third report. *WHO Tech. Rep. Ser.* No. 752.
- Wilson, K. & Grenfell, B.T. 1996 Generalised linear modelling for parasitologists. *Parasitol. Today* **13**, 33–38.

As this paper exceeds the maximum length normally considered for publication in *Proceedings B*, the authors have agreed to contribute towards production costs.

